The lattice location of Ni in diamond: a theoretical study

2004 J. Phys.: Condens. Matter 16 4567

(http://iopscience.iop.org/0953-8984/16/25/014)

INSTITUTE OF PHYSICS PUBLISHING JOURNAL OF PHYSICS: CONDENSED MATTER

J. Phys.: Condens. Matter **16** (2004) 4567–4578 PII: S0953-8984(04)78844-X

The lattice location of Ni in diamond: a theoretical study

J P Goss[1], P R Briddon[1], R Jones[2] and S Öberg[3]

[1] School of Natural Sciences, University of Newcastle upon Tyne, Newcastle upon Tyne NE1 7RU, UK
[2] School of Physics, The University of Exeter, Exeter EX4 4QL, UK
[3] Department of Mathematics, Luleå University of Technology, Luleå S-97187, Sweden

E-mail: J.P.Goss@ncl.ac.uk

Received 30 March 2004
Published 11 June 2004
Online at stacks.iop.org/JPhysCM/16/4567
doi:10.1088/0953-8984/16/25/014

Abstract

Experiment unambiguously shows substitutional nickel is present in as-grown synthetic diamond where Ni is present in the solvent–catalyst. There is less convincing evidence for the presence of an interstitial species. We present the results of first-principles calculations of the properties of substitutional and interstitial Ni in diamond. The formation energy and mobility of the interstitial species suggest that nickel will be predominantly of the substitutional form. We also present possible models for the trigonal 1.404 eV optical centre correlated with the NIRIM-2 paramagnetic defect.

1. Introduction

Ni is the most commonly observed transition metal (TM) impurity forming point defects in diamond, although Co has also been identified experimentally [1, 2], and there are more speculative assignments for other species (see for example [3], and references therein). Ni is typically seen in samples grown using the high temperature and high pressure technique where Ni is present in the solvent–catalyst, but also present in some natural material [4]. Ni gives rise to optical and magnetic signals, many of which are linked with other components such as N [5–13], B [14] and/or lattice vacancies [6–9]. Despite considerable effort, identifications of the electron paramagnetic resonance (EPR) and optical centres with microscopic structures remain controversial in many cases. Therefore we begin by presenting a brief review of selected experimental and theoretical results.

1.1. Experimental centres

The only unambiguously identified Ni-related defect is negatively charged substitutional nickel (Ni_s^-): the T_d, $S = 3/2$ EPR centre labelled W8 [15]. Observation of ^{13}C hyperfine structure

with sets of four and twelve neighbours is clearly indicative of the substitutional site. W8 has been linked with an acceptor level, $(-/0)$, at $E_c - 2.49 \pm 0.03$ eV [16, 17], optical absorption peaks at 2.51 eV and 1.88 eV, and a 2.56 eV luminescence band [16], although the 1.88 eV centre has low symmetry and may thus be connected with an additional component such as N [18], and the 2.56 eV emission has a complex structure which is difficult to attribute to T_d Ni_s^- [19].

W8 requires the presence of donors, and indeed Ni_s^- is observed in material containing substitutional nitrogen (N_s). However, where [N_s] is low and/or boron added, W8 and related optical centres disappear and other dominant signatures are seen [20, 21]: in particular, the 1.404 eV doublet (seen in absorption and luminescence). This has been linked to the NIRIM-2 EPR centre [22], and in this paper we refer to the underlying defect as NIRIM-2. Seen alongside NIRIM-2 is the NIRIM-1 EPR centre, which is isotropic above around 20 K, but exhibits a lower symmetry at temperature 4 K [21]. NIRIM-1 appears to be less thermally stable than NIRIM-2: the NIRIM-1 signal decreases upon annealing to 1900 °C whereas NIRIM-2 appears insensitive to this heat treatment [23]. The changes at 1900 °C might be due to NIRIM-1 breaking up or diffusing at these temperatures, or an increase in the mobility for a second impurity (such as N or B) or might reflect changes in the Fermi level. If 1900 °C represents a diffusion temperature, this suggests a substantial barrier. The initial assignments for NIRIM-1 and NIRIM-2 were Ni_i^+ and Ni_i^+ perturbed by a nearby defect such as a vacancy, respectively [21]. Subsequent detailed analysis of the magnetic circular dichroism in the optical absorption of the 1.404 eV doublet has lent support to the assignment of NIRIM-2 to Ni_i^+ [24], with one suggestion being Ni_i^+ 3.08 Å from a boron acceptor [25]. NIRIM-1 has been correlated with a donor level, $(0/+)$, at $E_c - 1.98 \pm 0.03$ eV [26].

Perhaps a crucial quality of the 1.404 eV optical system lies in an unusual polarization: the defect responsible for the optical transition is preferentially aligned along one specific $\langle 111 \rangle$ direction [20] associated with the $\{111\}$ growth sectors into which the Ni is preferentially incorporated [20, 27, 28]. Given the 1.404 eV system remains polarized from the growth conditions, it seems likely that the barrier to reorientation is substantial: if aligned at a temperature of $\sim$2000 K, this suggests a barrier in excess of 5 eV! Although this is possible for an isolated defect such as Ni_s or Ni_i, a more likely interpretation is that the defect is a complex of two or more components along the $\langle 111 \rangle$ axis formed preferentially in one specific orientation during growth.

Under illumination and where [N_s] is extremely low, the 1.404 eV doublet is partially suppressed and a new transition at around 1.22 eV is observed [29]. It is believed that this is a different charge state of the 1.404 eV centre, which involves a band edge, and it has been assigned to Ni_i^{2+} [30].

There are numerous other optical and Ni-related EPR centres. Many appear subsequent to heat treatments, suggestive of aggregation, especially in nitrogen-containing material [5]. A class of EPR centres labelled NE1–NE9 are most probably due to Ni situated at the centre of a di-vacancy with various numbers of N neighbours [9]. Of these, NE4, which is trigonal in symmetry, is believed to be the undecorated complex (Ni–V), and the $S = 1/2$ state in N-containing material suggests a negative charge state. NE4 is probably the same as AB1 [31].

1.2. Theory

A theory due to Ludwig and Woodbury (LW) [32] suggests that substitutional and interstitial TM species can be understood on the basis of the 3d electrons, split into e and t_2 states by the T_d crystal field of the host. For Ni_s, four electrons go into bonding combinations with the four neighbours, leaving $3d^6$, whereas Ni_i retains all ten electrons. The crystal field splitting

acts in opposite senses for Ni_s and Ni_i, leading to $e^4t_2^2$ and $t_2^6e^4$ configurations for Ni_s and Ni_i, respectively. LW's is a popular view of the electronic structure of TM ions, but has been found to be in agreement with experiment only in some cases and cannot be generally applied (see for example [33]). However, it seems to be observed, at least superficially, for Ni in diamond.

There is some evidence of a small distortion to C_{3v} symmetry for Ni_s^0 and Ni_s^+ [34, 35], although other calculations suggest that no such distortions occur [36]. According to LW, Ni_s^0 and Ni_s^+ are Jahn–Teller systems, which is also true in the calculated $^3T_1$ and $^2T_2$ many-body symmetries [37]. However, the distortion to C_{3v} symmetry reported by Larico *et al* [34, 35] for Ni_s yields a many-body symmetry ^3E, which does not raise the orbital degeneracy and is therefore not Jahn–Teller in origin, although the energy saved is small (0.15 eV). Ni_s theoretically has both (0/+) and (−/0) levels around mid-gap [37, 34], and a double donor level in the bottom half of the band gap [37]. The small separation of the (−/0) and (0/+) levels has led to speculation that only Ni_s^- and Ni_s^+ would be seen experimentally [34].

The assignment of Ni_i^+ to NIRIM-2 requires a centre *statically* distorted from T_d to C_{3v}. Therefore, the T_d structure must be unstable and very high in energy or there must exist a large barrier between configurations. Some calculations have indeed found that Ni_i spontaneously moves from the T_d site along ⟨111⟩ [30, 34, 35, 38–42]. In particular, recent *ab initio* calculations [34, 35] indicate a distortion with Ni_i^+ moving 0.23 Å from the T_d site, accompanied by a 0.34 eV drop in energy. They also found a 0.60 eV barrier to convert the C_{3v} structure back to on-site. Other first-principles theoretical treatments suggest that there is no distortion, at least in the positive charge state required for paramagnetism [36, 37, 43]. In fact, why should such a distortion occur? T_d Ni_i^+ has a $t_2^6e^3$ configuration, and a distortion to C_{3v} does not raise the degeneracy [34]. Therefore the driving force for the distortion must be either spin–orbit or chemical re-bonding in origin. A distortion due to spin–orbit interactions is likely to be small, and in any case such terms are most typically neglected in the quantum-mechanical calculations. A small distortion appears inconsistent with the static trigonal symmetry of NIRIM-2, as seen with the preferential ⟨111⟩ orientation [20]. However, a small distortion *is* consistent with the isotropic symmetry of NIRIM-1 above 20 K. Although chemical re-bonding remains a possibility, since all carbon atoms are already fully bonded, such a distortion, especially one stable above 1900 K, most likely involves the breaking of C–C bonds and a strong interaction with the Ni ion. Such distortions have not been reported in the literature to our knowledge. Additionally, the calculated donor levels of Ni_i [34, 37] are far from the experimental NIRIM-1 donor level [26], suggesting that NIRIM-1 is not Ni_i^+.

Finally, there are theoretical treatments of Ni complexes with other components. Ni–V complexes indeed form the split-vacancy structure suggested by experiment [44, 45]. The (−/0) level of Ni–V has been estimated at $E_c - 4.3$ eV, supporting the view that NE4 is the negatively charged species in N-containing material [45], and the presence of a (0/+) level close to the valence band top admits the possibility of another paramagnetic form of the defect in p-type material. Ni–B complexes have also been treated theoretically [37, 43], yielding alternative trigonal Ni-related defects in B-doped material. Indeed, we have previously proposed an assignment for NIRIM-2 to Ni_s–B [43].

Given the contradictory nature of the evidence in the literature, and the apparent inconsistency between theoretical assignments and experimental evidence, we have re-examined the energetics of Ni_s, Ni_i and some trigonal Ni–X defects for low [N] material where NIRIM-1 and NIRIM-2 are observed.

2. Method

Local spin density functional calculations were carried out using AIMPRO (*Ab Initio* Modelling PROgram) [46] with periodic boundary conditions. We employ pseudopotentials [47, 48], with

the valence wavefunctions described using a basis of sets of independent s, p and d Gaussian orbitals with four different exponents sited at each atom site. Typically, a regular mesh of 2^3 **k**-points are used to sample the band structure [49], and the charge density is Fourier transformed using plane waves with an energy cut-off of 300 Ryd. The Ni basis set yields the lattice constant for bulk fcc Ni within 3% of experiment, and the carbon basis set reproduces the lattice constant and bulk modulus of diamond to within 1% and 5% respectively, with the band structure close to previously published results [50].

Electrical levels can be obtained using formation energies (E^{f}), defined as

$$E^{\mathrm{f}}(\mathrm{X}, q) = E^{\mathrm{Calc.}}(\mathrm{X}, q) - \sum(\mu_{\mathrm{i}}) - q(E_{\mathrm{v}}(\mathrm{X}, q) + \mu_{\mathrm{e}}) - \eta(\mathrm{X}, q) \tag{1}$$

where, for system X in charge state q, $E^{\mathrm{Calc.}}$ is the computed total energy, $E_{\mathrm{v}}(\mathrm{X}, q)$ is the location of the valence band top, μ_{i} and μ_{e} are the chemical potentials of the atoms and electrons respectively, and η is a correction term due to the periodic boundary conditions. However, there are a number of problems associated with such calculations [45]. Instead, for $(-/0)$ and $(0/+)$ levels we use an alternative approach utilizing a second system for alignment [45, 51]. Here we calculate the ionization energy or electron affinity of a bulk cell to represent E_{v} and E_{c}, respectively. Then, for example, the donor level with respect to E_{v} of system X is given by $[E(\mathrm{X}^0) - E(\mathrm{X}^+)] - [E(\mathrm{bulk}^0) - E(\mathrm{bulk}^0)]$. Additionally, we have adopted the convention that a positive binding energy represents a bound system; i.e. for the species A and B to form AB, the binding energy is $E^{\mathrm{b}}(\mathrm{AB}) = E^{\mathrm{f}}(\mathrm{A}) + E^{\mathrm{f}}(\mathrm{B}) - E^{\mathrm{f}}(\mathrm{AB})$.

Finally, we have calculated the modes of vibration by calculating the second derivitives of the total energy with respect to atomic positions typically for the impurity atoms and their immediate neighbours. The dynamical matrix is then constructed using these values, along with the remaining interactions being approximated from a simple valence force potential fitted to the first-principles derivitives of bulk diamond. This procedure is more accurate for modes of vibration above the bulk one-phonon maximum, but resonant modes can also be obtained approximately, especially where the bulk phonon density of states is low.

3. Results

3.1. Substitutional Ni

$\mathrm{Ni_s}$ was relaxed in a 64-atom cubic unit cell in charge states from −3 to +3, and we analysed the geometries, dilatation and electrical properties.

3.1.1. Geometry and volume relaxation. We find that relaxing geometries with lower than $\mathrm{T_d}$ symmetry results in structures indistinguishable from those obtained under a $\mathrm{T_d}$ constraint. Although this does not preclude a small distortion to lower symmetry, we conclude that such distortions must be small both in terms of the displacements of the atoms and the energy. This is broadly in line with recent studies using 54-atom fcc supercells [34]. However, that study indicated that for the +1 and neutral charge states, $\mathrm{Ni_s}$ relaxes to a $\mathrm{C_{3v}}$ structure with one Ni–C bond longer than the other three. We note that in these calculations the Γ point was explicitly included in the Brillouin-zone sampling in addition to a Monkhorst–Pack mesh. Since in general the full degeneracy of the gap states is only observed at Γ, such a sampling might be important in obtaining Jahn–Teller and other small distortions. We therefore performed calculations including the Γ point, but still find no propensity to distort from the $\mathrm{T_d}$ structure. It is not obvious why our results differ from those of Larico *et al*, but we note that our calculations are in larger supercells. Indeed, we have looked for distortions to $\mathrm{C_{3v}}$ in 216-atom cubic supercells, and find the same results as those determined in the 64-atom cell, i.e. Ni on site.

The presence of a large impurity atom[4] gives rise to considerable local distortion. The nearest neighbour bond lengths of Ni_s^0 are 1.75 Å, 15% larger than the bulk bond length. However, the displacement of the second-nearest neighbours is only around 1%, suggesting that the 64-atom cell is large enough to model the atomic displacements around Ni_s. For the various stable charge states of the defect the Ni–C bond lengths vary by less 0.01 Å. Ni_s^0 in 128-atom (fcc) and 216-atom (cubic) supercells yields local geometries very close to that found in the smaller cell: the Ni–C lengths differ by less than 0.02 Å.

We find that the spin states for the different charge states follow Hund's rule, so the double-positive, positive, neutral and negative defects have $S = 0$, $S = 1/2$, $S = 1$ and $S = 3/2$, respectively. Here the spin splitting for Ni_s^0 has been approximated by treating the $S = 1$ and $S = 0$ configurations as single-determinantal wavefunctions, yielding a spin splitting of 0.3 eV. Such a procedure is not precise, but we note that previous calculations have also yielded a $S = 1$ ground state [37].

One might expect a net lattice expansion due to the presence of Ni_s. We minimized the energy with respect to the lattice constant, and for Ni_s^0 the volume dilation is $1.4V_{ref}$ ($V_{ref} = a_0^3/8$), similar to that of the single self-interstitial [52]. The changes in bond lengths after increasing a_0 are <0.5%. The volume change is accompanied by a 0.2 eV drop in $E^f(Ni_s)$ for all charge states.

3.1.2. Vibrational modes. The compression of lattice around Ni_s^- might be expected to give rise to vibrational modes that lie above the one-phonon maximum. However, we note that the displacement of the surrounding atoms does not lead to particularly short C–C bonds: the back-bonds are shortened by just 3%. Indeed, our calculations yield no high frequency vibrations, but a T_2 symmetry mode which is strongly localized with the Ni atom lies around 270 cm^{-1}. Where the calculation is performed on a volume relaxed supercell, this mode is shifted down in frequency by a negligible amount. Increasing the number of atoms for which the energy derivitives were explicitly calculated to include the second-neighbour shell also has no significant effect on these modes. There are less strongly localized modes also present, notably around the 1000–1200 cm^{-1} range. These modes calculated at 1000, 1030 and 1220 cm^{-1} are mostly associated with the motion of the four nearest neighbours, and are of T_2, A_1 and E symmetry. No other modes of vibration are more than 30% localized on the Ni and four neighbouring carbon atoms, but modes around 500 and 900 cm^{-1} might also be associated with the defect. Figure 1 shows all modes calculated for the system. We note that the 2.56 eV emission band has phonon sidebands at around 200, 370, 1010 and 1190 cm^{-1}. These modes have been interpreted as characteristic of a di-nickel defect [3], but we find them to be broadly consistent with the modes of a single Ni_s.

3.1.3. Donor and acceptor states of Ni_s. We have calculated the electrical levels of Ni_s using the electron affinity and ionization energies of a bulk cell as described in section 2. The acceptor level is located at $E_c - 2.5$ eV, in excellent agreement with experiment, and a donor level lies at $E_v + 2.2$ eV. The acceptor levels calculated for both the 128- and 216-atom cells lie at $E_c - 2.4$ eV, implying that this value is already reasonably converged for the 64-atom cell.

Previous calculations using the formation energy approach predicted Ni_s to have a double donor level deep in the band gap [37]. However, we do not find this to be the case. Using the formation energy approach [45], and including a correction for the periodic boundary condition [53], we predict that the (2+/+) level would be close to the valence band top.

[4] The covalent radius of Ni at 121 pm is 57% larger than that of carbon (77 pm).

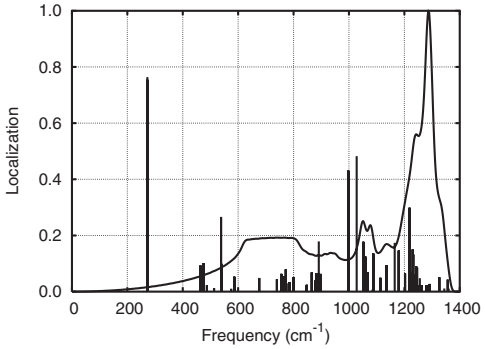

Figure 1. Modes of vibration (vertical lines) for Ni_s^- with line heights representing the localization on the central five atoms. Also plotted is the calculated bulk phonon density of states.

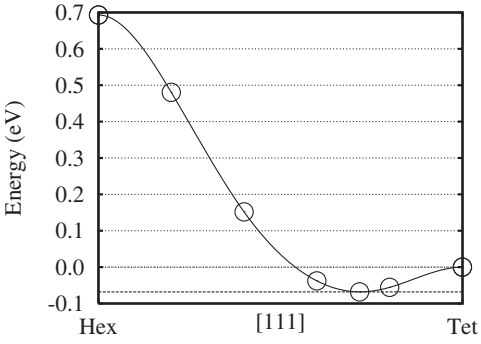

Figure 2. The migration barrier for Ni_i in diamond (eV). Calculated points are shown by the circles, with the solid curve a guide to the eye. The horizontal, dashed line indicates the minimum at around −0.07 eV.

3.2. Interstitial Ni

3.2.1. Geometry. For T_d Ni_i^0, LW indicate a $t_2^6e^4$ configuration, i.e. a $^1A_1$ ground state. Ni_i strongly perturbs the surrounding cage, with the Ni–C separations being 1.73 and 1.88 Å to the four nearest and six next nearest neighbours, respectively, i.e. a 13% and 7% expansion when compared to the unrelaxed interstitial site. The third-neighbour shell is displaced by less than 1%. These results are similar to those of [34].

However, when the T_d constraint is relaxed and the Ni atom displaced along ⟨111⟩ away from one of the four carbon neighbours, the energy is lowered by around 70 meV. We also find this distortion in a 128-atom supercell with the same energy saving. We conclude that there could be a distortion to C_{3v} symmetry, but the driving force is not clear since it cannot be a simple Jahn–Teller effect in origin due to the orbitally non-degenerate ground state. Lowering the symmetry to C_{1h} reduces the total energy further by around 85 meV. The resultant geometry contains several elongated C–C bonds, one of which is effectively broken at 2.16 Å. The presence of the broken bond leads to an unoccupied Kohn–Sham level close to E_c, admitting the possibility of Ni_i^0 capturing an electron. Indeed, this C_{1h} structure is strongly preferred in the negative charge state, leading to a $(-/0)$ level very close to E_c. The small energy differences between the planar, trigonal and tetrahedral structures leads one to suspect that there may be other low symmetry perturbations with similar total energies, but that the symmetry at elevated temperatures would be close to tetrahedral.

In the positive charge state, we find that these distortions are unstable, and the on-site structure has the lowest total energy.

3.2.2. Electrical levels of Ni_i. The assignment of isolated Ni_i to a $S = 1/2$ centre requires Ni_i to be charged. Using the bulk ionization energy as a marker, in line with previous theory [37], shows that Ni_i does not have a *deep* $(-/0)$ level, but does possess a $(0/+)$ level at $E_v + 1.5$ eV. Previous calculations placed the donor level at $E_v + 2$ eV [37] and $E_v + 0.9$ eV [34].

Hence the only candidate for an $S = 1/2$ EPR isolated Ni_i centre is Ni_i^+. In this charge state, in contrast to [34] but in agreement with [37], we find no stable trigonal or other distortion. It should be noted that the one-electron picture for the on-site defect ($t_2^6e^3$) *is* a Jahn–Teller system but, as pointed out above, a distortion to C_{3v} symmetry does not raise the degeneracy in the absence of spin–orbit effects, and in any case is unlikely to lead to a static distortion, as required to explain the polarization of NIRIM-2.

Thus, on the basis of the computed geometry, the assignment of NIRIM-1 to Ni_i^+ seems more reasonable than that of NIRIM-2. However, the theoretical (0/+) level must be in considerable error for this assignment to be correct. Alternatively the experimental value might be referenced to the wrong band edge, i.e. the level may lie at $E_v + 1.98 \pm 0.03$ eV rather than $E_c - 1.98 \pm 0.03$ eV [26], or reflect a recharging of NIRIM-1 from another defect.

3.2.3. Migration barrier. An additional, high symmetry structure for Ni_i was also considered. The Ni atom was placed at the hexagonal interstitial site (H), corresponding to the mid-point between two T_d sites. Such a structure often represents the saddle point for diffusion, and using this assumption we estimate a migration barrier at 0.8 eV, a value which is insensitive to the supercell size (64- and 128-atom cells). This surprisingly low value is much smaller than the values derived using more approximate methods [40, 42] where the relaxation of material surrounding the defect was apparently incomplete. The calculated barrier height is slightly larger in the 1+ and 2+ charge states at 0.9 and 1.0 eV, respectively, but the values remain relatively small, especially in the context of the growth temperature.

We have also examined the intermediate stages between Ni_i at the T and H sites. (For simplicity we assume that the trajectory for the interstitial species is along the ⟨111⟩ directions and neglect the effect of the off-axis lower symmetry structures.) The diffusion barrier profile is shown in figure 2. We conclude that at 1900 °C, where NIRIM-1 is reduced in intensity, Ni_i is highly mobile. One might then interpret this annealing pattern as the loss of Ni_i^+ to some traps in the samples, supporting the view that NIRIM-1 is Ni_i^+. However, care must be taken in such a conclusion, since the loss of NIRIM-1 at high temperatures might simply reflect a change of the centre to a diamagnetic charge state, or the trapping of another defect that is mobile at elevated temperatures. Furthermore, one would expect a barrier around 1 eV to correspond to diffusion at a much lower temperature than 1900 °C.

3.2.4. Volume expansion. At the H site the six equivalent Ni–C separations are 1.71 Å, compared to 1.73 Å in the T_d case. Both structures impact greatly on the surrounding lattice, and to examine this in more detail we relaxed the volume of the 64-atom supercells as with Ni_s. In all cases the total energy dropped considerably, but the relative energies of the different symmetries remained approximately the same. The variation of total energy with volume dilation is shown in figure 3, with the difference in the minima for the C_{3v} and 'hexagonal' structures equal to 0.65 eV. Figure 3 also indicates that the volume displaced by the Ni_i in the lattice is considerably larger than the $1.4V_{ref}$ of Ni_s: Ni_i displaces $\sim 2.5V_{ref}$. This displacement reflects the difficulty of insertion of Ni_i into the compact diamond lattice.

3.2.5. Vibrational modes. As with Ni_s^- we have estimated the vibrational properties of the C_{3v} symmetry Ni_i^0. The large volume displaced by Ni_i^0 reflects a large impact on the local environment, leading to local vibrational modes with E and A_1 symmetry, calculated to lie around 1430 cm^{-1}. These local modes are all associated with vibrations of the back-bonds of the three nearest C atoms. For the tetrahedral Ni_i^+, there are T_2 and A_1 local modes in the same frequency region. A vibration on the Ni atom lies around 180–200 cm^{-1}, depending on the charge state. We note that there are no such low frequency modes associated with the 1.404 eV centre. However, there are experimentally observed modes around 400, 800, 1020 and 1330 cm^{-1} [3], for which there are no clearly identifiable modes from our model Ni_i^+.

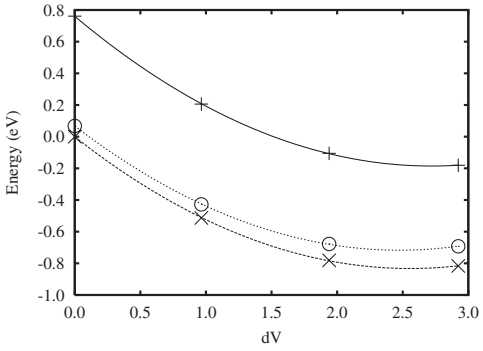

Figure 3. Dilation (dV) of the three Ni_i defects in the 64-atom supercell. dV is in units of the volume per host atom, $a_0^3/8$. Symbols +, × and O refer to the hexagonal, C_{3v} and T_d structures, respectively.

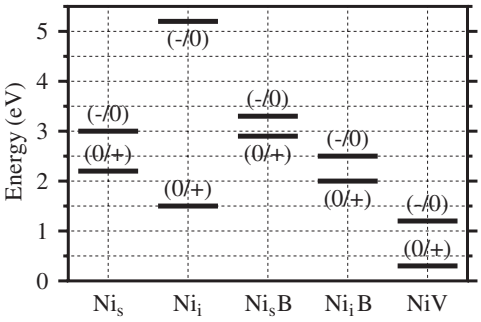

Figure 4. A schematic representation of the location of the donor and acceptor levels for Ni_s, Ni_i, Ni_s–B, Ni_i–B and Ni–V, as referenced against the bulk ionization energy and electron affinity, respectively.

3.3. Comparison of Ni_s and Ni_i

We find that the formation energies (equation (1)) of Ni_s^0 and Ni_i^0 differ by more than 7 eV. This is in stark contrast to the results of Gerstmann *et al* [37], who found the neutral species to be separated by around 1.2 eV, but with Ni_i being the lower in energy. However, more recent Hartree–Fock [54] and DFT [34] calculations also place the interstitial site much higher in energy than Ni_s.

The significantly higher formation energy of Ni_i coupled with the low activation barrier to diffusion can be interpreted as rendering isolated Ni_i unstable: for typical high pressure and high temperature growth the equilibrium $[Ni_s]$:$[Ni_i]$ should be ten or more orders of magnitude, and mobile Ni_i should be trapped at impurity sinks and/or diffuse out of the material during growth.

3.4. Ni–B complexes

If Ni_i is mobile as we predict, it will either be lost to the growing surface or trapped by some internal sink. If lattice vacancies are present, which seems likely given the temperature and pressure of synthesis, this would lead to immobile Ni_s. (It seems reasonable to assume that Ni_s is immobile since concerted exchange processes have very large activation energies.) Alternatively, Ni_i might bind with a substitutional impurity, such as boron. This possibility is significant in that the formation of many centres involving Ni, such as NIRIM-1 and NIRIM-2, seems to be enhanced by the addition of boron to the material, and indeed one model for the NOL1 EPR centre is a nearest neighbour Ni_s–B pair [25]. We have therefore examined the structure and properties of Ni–B pairs.

We find that B relaxes away from the Ni sites. For Ni_s–B the Ni–B bond length is around 0.2% longer than the Ni–C bonds. However, the Ni–B pair move along [111] such that the B atom becomes close to co-planar with its three carbon neighbours. This is enhanced further in the positive charge state where the Ni–B bond length is 1.77 Å, 2% longer than the Ni–C distance.

The binding energy of B_s and Ni_s is 0.9, 0.5 and 0.3 eV in the negative, neutral and positive charges states, respectively. The value for $(Ni_s–B)^+$ is in reasonable agreement with [37]. Despite the modest binding energies, the activation energy for dissociation is likely to be high

and the complex can therefore be considered a stable centre once formed, essentially frozen into the lattice.

For Ni_i–B, the Ni–B bond length is also slightly longer (∼0.01%) than the three Ni–C nearest neighbour distances. The binding energy for this complex is 0.8 eV, close to the value of 0.95 eV found previously for this pair [37]. We can then estimate the barrier to dissociation for the pair to be the sum of the binding and migration energies, i.e. ∼1.7 eV. In the positive and negative charge states the binding energies are estimated to be 1.7 and 0.5 eV, respectively. It therefore seems unlikely that this structure would be stable enough under the growing conditions to form in large quantities. An alternative trigonal structure where a carbon site lies between Ni_i and boron is calculated to be unbound with respect to isolated Ni and boron, at least in the neutral charge state, although the inter-nuclear separation is 3.2 Å, close to the value of 3.08 Å predicted in the recent model of NIRIM-2 of Baker [25].

The electronic configuration of Ni_i–B is unclear due to the resonance of the levels derived from the Ni_i t_2 states with the valence band: only the e^3 level is present in the band gap. However, the symmetry and the ^2E ground state are consistent with those of the 1.404 eV optical centre.

Using the same approach for the electrical levels as for isolated Ni_i and Ni_s, the single acceptor and donor levels of Ni_s–B are calculated to lie around $E_c - 2.6$ eV and $E_v + 2.3$ eV, respectively, and Ni_i–B has (0/+) and (−/0) levels at $E_v + 2.0$ eV and $E_c - 3.0$ eV, respectively.

It seems unlikely that a thermally stable trigonal defect with $S = 1/2$ can be made up by complexing Ni_i with boron, but Ni_s–B in the neutral charge state might be a candidate if such pairs are grown in. Ni_s acts as a donor and B_s as an acceptor, effectively yielding Ni_s^+–B_s^-. Ni can then be viewed as $3d^5$, with the unpaired electron likely to be associated more with the Ni atom than boron. Indeed, a Mulliken bond population analysis of the ^2E state of $(Ni_s–B)^0$ suggests that the unpaired electron has 47% and 12% localization on the Ni and on each of the C neighbours, respectively. There is less than 2% on the B atom, and it is possible that it would be difficult to resolve the presence of the B atom experimentally.

The electronic structure of Ni_s–B is $e^4e^1a_1^0$, in line with LW's work where the t_2 level is split by the trigonal crystal field. Possible excited states would then be $e^4e^0a_1^1$ ($^2A_1$) and $e^3e^2a_1^0$ ($^2A_1$, $^2A_2$, $^4A_2$ and ^2E symmetries). In the Kohn–Sham spectrum at the Brillouin-zone centre the e and a_1 levels associated with the t_2 Ni_s levels are split by around 1.2 eV, and the $(e^4e^1a_1^0) \rightarrow (e^4e^0a_1^1)$ transition represents $^2E \rightarrow {}^2A$, as required for the 1.404 eV doublet from the uniaxial stress and Zeeman experiments [55]. If the assignment of the 1.404 eV system to (Ni_s–B) was correct, the 1.22 eV optical transition could logically then arise from $(Ni_s–B)^+$, consistent with the type of material in which this latter optical feature is seen. Furthermore, since the migration and reorientation barriers for Ni_s–B are likely to be large, this defect is consistent with the high thermal stability and orientational polarization associated with NIRIM-2 and the 1.404 eV optical doublet.

Both Ni_i–B_s and Ni_s–B_s are predicted to give rise to characteristic vibrational modes. In both cases they strongly resemble those of the Ni component as described above. Additionally, the high frequency Ni_i–B_s mode shows a strong coupling with the B atom, and should exhibit isotopic structure in any resulting optical signal. Ni_s–B_s also possesses a strongly localized mode around 950 cm^{-1} associated with the B atom. Due to the nature of the calculations it is impossible to correlate vibrations of either structure with experimental peaks with any degree of certainty. Since both possess modes consistent with the 1.404 eV centre, neither can be ruled out on the basis of these data.

Finally, we note that the unusual anisotropy of the NIRIM-2 g-tensor is viewed to be most consistent with a $3d^9$ configuration. However, it is not clear that the anisotropy is unequivocally *inconsistent* with an assignment to (Ni_s–B_s).

3.5. The vacancy–nickel complex

We finally consider the complex consisting of a lattice vacancy and Ni_s. The defect adopts the D_{3d} split-vacancy configuration, similar to that of the vacancy–silicon complex in diamond [6, 56, 57]. The NE4 EPR centre is believed to arise from $(Ni–V)^-$ in N-containing material, and it is unclear whether the centre may adopt other charge states.

The differences in formation energies of Ni_s and Ni–V $[E^f(Ni_s) - E^f((Ni–V))]$ are 0.5, 2.0 and 4.1 eV for the positive, neutral and negative charge states, respectively, with the formation energies defined by equation (1). The value for $(Ni–V)^0$ is close to that obtained from other *ab initio* calculations [54]. These energy differences can be related to a binding energies of Ni_s and V by including the formation energy of the lattice vacancy, i.e. $E^b(Ni–V) = E^f(Ni_s) + E^f(V) - E^f(Ni–V)$. Using $E^f(V) = 6$ eV from quantum Monte Carlo calculations [58], the implication is that the binding energy of (Ni–V) is considerable, and greater than 10 eV in the negative charge state correlated with the NE4 EPR centre.

$(Ni–V)^0$ has an electronic configuration characterized by the gap states $e_u^2 e_g^0$, leading to three multiplets. We have calculated the energy of the $S = 1$ configuration relative to that of an admixture of the two spin singlets, and we find that the $S = 1$ state is just 0.2 eV lower in energy. Given the potentially large multiplet splittings, it is not possible to determine with any certainty whether the ground state of $(Ni–V)^0$ is paramagnetic. Resonant with the valence band is a state which is ∼80% localized on the Ni atom and has a_{1g} symmetry. This admits the possibility of an $a_{1g} \rightarrow e_u$ transition, in line with the symmetries obtained by uniaxial stress for the 1.404 eV system. The separation of the two Kohn–Sham levels potentially involved in this optical transition is around 1.5 eV, in reasonable agreement with the experimental line energy. However, such a calculation represents a very crude estimate of the optical excitation energy for such a transition, and the agreement may well be fortuitous.

(Ni–V) possesses an acceptor level calculated at $E_c - 4.3$ eV, and, in equilibrium with nitrogen donors, it will therefore be negatively charged and paramagnetic, consistent with the observation of NE4 in N-containing material. A donor level lies at around $E_v + 0.3$ eV, close to the boron acceptor level. However, due to the uncertainty in the calculation we cannot be certain as to whether the centre can be positively charged in p-type diamond. If it can, then this defect would be a statically trigonal (D_{3d}) defect with an effective spin of $S = 1/2$ in p-type diamond. We note that the ^2E_u ground state of the trigonal defect is unstable against a Jahn–Teller distortion.

The vibrational modes of $(Ni–V)^0$ consist chiefly of modes around 250 cm^{-1} with A_{2u} and E_u symmetries separated by around 10 cm^{-1}. The space afforded to Ni in the split vacancy reduces the strain and thus does not lead to any clear local modes, and it is not obvious that this defect could give rise to the vibronic peaks seen, for example, in the 1.404 eV system.

However, the positively charged defect is at least consistent with a number of the observations regarding NIRIM-2, namely the symmetry and effective spin, and is only present in material where the Fermi level is close to the valence band. Furthermore, the Kohn–Sham levels suggest that the centre is potentially optically active. The suggestion that NIRIM-2 might arise from the split-vacancy structure has been made previously [25], but for the −3 charge state which we view as being unstable.

4. Summary and conclusions

We have performed *ab initio* calculations examining the formation energy of Ni_s and Ni_i in diamond in various charge states. The calculated acceptor level for Ni_s is in good agreement with experiment. This, along with the calculated properties of bulk Ni gives us confidence in the properties of Ni in diamond.

The donor and acceptor levels calculated for a range of Ni-related defects are summarized in figure 4.

We find that Ni_i has an activation barrier to diffusion of less than 1 eV, implying that this defect would be *highly mobile* under the high temperature, high pressure conditions of diamond synthesis. Therefore, since the equilibrium solubility of Ni is relatively small, the only Ni_i species that would be present in such samples would be those complexed with another defect with a large binding energy. We have found no such complexes.

We note that unlike that for Ni_s^-, the *experimental* evidence for isolated Ni_i is indirect. In particular, we are unable to support the correlation of NIRIM-2 with Ni_i^+ [34] for two key reasons. First, we do not observe any distortion of Ni_i in the paramagnetic state, and hence the symmetry of Ni_i^+ is *inconsistent* with experiment. Secondly, even if there is a distortion as with [34], the polarization of the 1.404 eV optical system suggests a defect that cannot reorient at the growth temperature, inconsistent with small displacements of the Ni atom: Larico *et al* report a reorientation barrier of $\leqslant$0.6 eV. Instead, we conclude that NIRIM-2 is not a simple Ni_i defect, but instead must be due to a trigonal Ni–X complex. One possibility is that X is a lattice vacancy in p-type material. Alternatively, we favour the model of X being boron, with the (Ni_s–B) complex possessing favourable symmetry, electronic and optical characteristics, as well as a very small spin density on the B atom. This model has been suggested previously from our cluster-based calculations [43]. However, this assignment is at odds with [24] and [25], which depend on the interpretation of the expected behaviour of the spin–orbit parameters for Ni in diamond.

The model for NIRIM-2 made up from Ni_i^+ around 3 Å from a substitutional boron is inconsistent with our results which indicate that such a complex is unbound. The nearest neighbour Ni_i–B pair has the correct ^{2}E ground state, but is weakly bound, inconsistent with the annealing properties of NIRIM-2. The mobility of isolated Ni_i along with the donor level lying low in the band gap means that we cannot support the assignment of Ni_i^+ to NIRIM-1, and we favour our earlier assignment of NIRIM-1 to Ni_s^+ [43], which has received some support [25, 34].

Acknowledgments

We thank J M Baker and K Iakoubovskii for helpful discussions.

References

[1] Lawson S C, Kanda H, Watanabe K, Kiflawi I, Sato I and Collins A T 1996 *J. Appl. Phys.* **79** 4348–57
[2] Twitchen D J, Baker J M, Newton M E and Johnston K 2000 *Phys. Rev.* B **61** 9–11
[3] Zaitsev A M 2000 *Phys. Rev.* B **61** 12909–22
[4] Iakoubovskii K and Adriaenssens G J 2002 *Diamond Relat. Mater.* **11** 125–31
[5] Lawson S C and Kanda H 1993 *J. Appl. Phys.* **73** 3967–73
[6] Nadolinny V and Yelisseyev A 1994 *Diamond Relat. Mater.* **3** 1196–200
[7] Yelisseyev A and Nadolinny V 1995 *Diamond Relat. Mater.* **4** 177–85
[8] Nadolinny V A, Yelisseyev A P, Yuryeva O P and Feygelson B N 1997 *Appl. Magn. Reson.* **12** 543–54
[9] Nadolinny V A, Yelisseyev A P, Baker J M, Newton M E, Twitchen D J, Lawson S C, Yuryeva O P and Feigelson B N 1999 *J. Phys.: Condens. Matter* **11** 7357–376
[10] Nazaré M H, Rino L M and Kanda H 1995 *Mater. Sci. Forum* **196–201** 73–8
[11] Neves A J, Nazaré M H, Lopes J C and Kanda H 1999 *Physica* B **273/274** 636–9
[12] Mashkovtsev R I and Pal'yanov Y N 1999 *Solid State Commun.* **111** 397–402
[13] Neves A J, Pereira R, Sobolev N A, Nazaré M H, Gehlhoff W, Näser A and Kanda H 2000 *Diamond Relat. Mater.* **9** 1057–60
[14] Nadolinny V A, Baker J M, Newton N E and Kanda H 2002 *Diamond Relat. Mater.* **11** 627–30

[15] Isoya J, Kanda H, Norris J R, Tang J and Bowman M K 1990 *Phys. Rev.* B **41** 3905–17
[16] Hofmann D M, Ludwig M, Christmann P, Volm D, Meyer B K, Pereira L, Santos L and Pereira E 1994 *Phys. Rev.* B **50** 17618–20
[17] Pereira R N, Gehlhoff W, Sobolev N A, Neves A J and Bimberg D 2001 *J. Phys.: Condens. Matter* **13** 8957–64
[18] Nazaré M H, Rino L M and Kanda H 1996 *Mater. Sci. Eng.* A **209** 302–5
[19] Pereira E, Pereira L, Hofmann D M, Stadler W and Meyer B K 1995 *Radiat. Eff. Defects Solids* **135** 641–6
[20] Collins A T 1989 *J. Phys.: Condens. Matter* **1** 439–50
[21] Isoya J, Kanda H and Uchida Y 1990 *Phys. Rev.* B **42** 9843–52
[22] Pawlik T, Noble C and Spaeth J M 1998 *J. Phys.: Condens. Matter* **10** 9833–40
[23] Pereira R N, Gehlhoff W, Neves A J, Sobolev N A, Rino L and Kanda H 2003 *J. Phys.: Condens. Matter* **15** S2941–9
[24] Mason P W, Ham F S and Watkins G D 1999 *Phys. Rev.* B **60** 5417–27
[25] Baker J M 2003 *J. Phys.: Condens. Matter* **15** S2929–40
[26] Pereira R N, Gehlhoff W, Neves A J and Sobolev N A 2003 *J. Phys.: Condens. Matter* **15** 2493–505
[27] Collins A T, Kanda H and Burns R C 1990 *Phil. Mag.* B **61** 797–810
[28] Burns R C, Cvetkovik V, Dodge C N, Evans D J F, Rooney M L T, Spear P M and Welbourn C M 1990 *J. Cryst. Growth* **104** 257–79
[29] Lawson S C, Kanda H and Sekita M 1993 *Phil. Mag.* B **68** 39–46
[30] Lowther J E 1995 *Phys. Rev.* B **51** 91–6
[31] Gehlhoff W and Pereira R N 2002 *J. Phys.: Condens. Matter* **14** 13751–60
[32] Ludwig G W and Woodbury H H 1962 *Electron Spin Resonance in Semiconductors* (*Solid State Physics* vol 13) (New York: Academic)
[33] Zunger A 1986 *Electronic Structure of 3d Transition-Atom Impurities in Semiconductors* (*Solid State Physics* vol 39) (New York: Academic)
[34] Larico R, Assali L V C, Machado W V M and Justo J F 2004 *Appl. Phys. Lett.* **84** 720–2
[35] Larico R, Justo J F, Machado W V M and Assali L V C 2003 *Physica* B **340–342** 84–8
[36] Gerstmann U, Amkreutz M and Overhof H 1999 *Physica* B **273/274** 632–5
[37] Gerstmann U, Amkreutz M and Overhof H 2000 *Phys. Status Solidi* b **217** 665–84
[38] Paslovsky L and Lowther J E 1991 *Solid State Commun.* **80** 541–3
[39] Paslovsky L and Lowther J E 1992 *J. Phys.: Condens. Matter* **4** 775–84
[40] Paslovsky L and Lowther J E 1993 *J. Phys. Chem. Solids* **54** 243–56
[41] Paslovsky L, Lowther J E, Nam T L and Keddy R J 1993 *J. Lumin.* **55** 167–72
[42] Yang J, Zhang M and Wang K 1994 *Phys. Rev.* B **49** 15525–30
[43] Goss J, Resende A, Jones R, Öberg S and Briddon P R 1995 *Mater. Sci. Forum* **196–201** 67–71
[44] Johnston K and Mainwood A 2003 *Diamond Relat. Mater.* **12** 516–20
[45] Goss J P, Briddon P R, Sque S J and Jones R 2004 *Diamond Relat. Mater.* **13** 684–90
[46] Jones R and Briddon P R 1998 *The Ab Initio Cluster Method and the Dynamics of Defects in Semiconductors* (*Semiconductors and Semimetals* vol 51A) (Boston, MA: Academic) chapter 6
[47] Bachelet G B, Hamann D R and Schlüter M 1982 *Phys. Rev.* B **26** 4199–228
[48] Troullier N and Martins J L 1991 *Phys. Rev.* B **43** 1993–2006
[49] Monkhorst H J and Pack J D 1976 *Phys. Rev.* B **13** 5188–92
[50] Liberman D A 2000 *Phys. Rev.* B **62** 6851–53
[51] Jeong J W and Oshiyama A 2001 *Phys. Rev.* B **64** 235204
[52] Goss J P, Jones R and Briddon P R 2002 *Phys. Rev.* B **65** 035203
[53] Makov G and Payne M C 1995 *Phys. Rev.* B **51** 4014–122
[54] Watkins M and Mainwood A 2003 *J. Phys.: Condens. Matter* **15** S2913–27
[55] Nazaré M H, Neves A J and Davies G 1991 *Phys. Rev.* B **43** 14196–205
[56] Goss J P, Jones R, Breuer S J, Briddon P R and Öberg S 1996 *Phys. Rev. Lett.* **77** 3041–4
[57] Johnston K and Mainwood A 2002 *Diamond Relat. Mater.* **11** 631–4
[58] Hood R Q, Kent P R C, Needs R J and Briddon P R 2003 *Phys. Rev. Lett.* **91** 076403